ChemComm

Intermediate snapshots of a 116-nuclear metallosupramolecular cage-of-cage in a homogeneous single-crystal-to-single-crystal transformation

Journal:	*ChemComm*
Manuscript ID	CC-COM-04-2021-002219.R1
Article Type:	Communication

COMMUNICATION

Intermediate snapshots of a 116-nuclear metallosupramolecular cage-of-cage in a homogeneous single-crystal-to-single-crystal transformation

Received 00th January 20xx,
Accepted 00th January 20xx

DOI: 10.1039/x0xx00000x

Benny Wahyudianto,[a] Kento Imanishi,[a] Tatsuhiro Kojima,[a] Nobuto Yoshinari,[a] and Takumi Konno[a]*

Soaking crystals of an $Au^{I}_{72}Cd^{II}_{40}Na^{I}_{4}$ cage-of-cage in aqueous $Co(NO_3)_2$ afforded an analogous $Au^{I}_{72}Co^{II}_{44}$ cage-of-cage, accompanied by the exchange of Na^{I} and Cd^{II} by Co^{II} with retention of the single crystallinity. The homogeneous progress of the transformation led to the direct observation of intermediate species by single-crystal X-ray crystallography.

Post-synthesis in the solid state is a modern synthetic methodology that has attracted increasing attention in material science for the past decade.[1] This is because new chemical species with intriguing architectures and properties, which are difficult to obtain by direct syntheses in solution, can be produced by this method. In some cases, post-synthetic reactions proceed with maintaining the single crystallinity of the precursors in a single-crystal-to-single-crystal (SCSC) transformation process, which allows us to gain structural information on the final reaction products using single-crystal X-ray crystallography.[2] Recently, an X-ray snapshot technique based on multiple diffraction measurements of a target crystal has been applied for monitoring SCSC transformation reactions to visualize the reaction intermediates.[3] This technique requires a high homogeneity of crystals in the course of the SCSC process, and thus, reports on X-ray snapshot analysis are limited to several examples, such as photochemical reactions,[4] spin crossover events,[5] adsorption/desorption of small guest molecules,[6] and substitution reactions.[7]

As one of the categories of the post-synthetic approach, SCSC metal exchange (transmetallation) reactions of crystalline compounds, which provide concomitant changes in structures, reactivities, and physical properties, have recently been developed in the field of coordination chemistry.[8] The reactions of this type involve two main processes: (i) a diffusion process in which a secondary metal ion (M2) approaches a metal ion

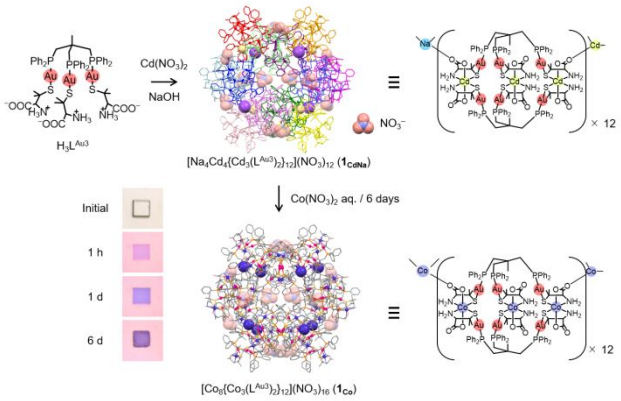

Scheme 1. Schematic of the synthetic route to $\mathbf{1}_{CdNa}$ and $\mathbf{1}_{Co}$.

(M1) in the reaction centre by solution diffusion and (ii) a transmetallation process in which M1 is replaced by M2. It has been recognized that the diffusion process is commonly slower than the transmetallation process, affording hetero-epitaxial crystals of the core-shell type in intermediate states.[8b] This prevents the observation of intermediate states via the X-ray snapshot technique, providing information about only the structural difference between the initial and final states. A closely related example of the structural characterization of a mixed-metal intermediate species by single-crystal X-ray crystallography has been reported by Zaworotko *et al*.[8d] In this case, however, a mixed-metal (Cd^{II}/Cu^{II}) species was obtained as a thermodynamically stable product by soaking crystals of a metal-organic framework (MOF) containing Cd^{II} centres in a mixture solution of Cd^{2+} and Cu^{2+} ions, rather than as an intermediate species formed by the use of only Cu^{2+} ions. W. Meng *et al.* reported an MOF system containing Zn^{II} centres, which shows homogeneous SCSC transmetallation by Cu^{2+} ions, but they detected a mixed-metal (Zn^{II}/Ni^{II}) intermediate state based on magnetic measurements and DFT calculations, rather than single-crystal X-ray diffraction measurements.[8e] Thus, the direct observation of intermediate species in an SCSC transmetallation event by single-crystal X-ray crystallography

[a] *Department of Chemistry, Graduate School of Science, Osaka University, Toyonaka, Osaka 560-0043, Japan*

† Electronic Supplementary Information (ESI) available: Experimental detail, PXRD, and IR, diffuse reflectance, and CD spectra, as well as crystal structures and crystallographic data. CCDC 2054688-2054595. See DOI: 10.1039/x0xx00000x

has rarely been reported, and obtaining their X-ray snapshots is a considerable challenge in materials science.

As part of our research on the creation of a new class of heterometallic coordination compounds using functional digold(I) and trigold(I) metalloligands, H_2L^{Au2} = $[Au_2(dppe)(D\text{-}Hpen)_2]$ and H_3L^{Au3} = $[Au_3(tdme)(D\text{-}Hpen)_3]$ (dppe = 1,2-bis(diphenylphosphino)ethane, tdme = 1,1,1-tris(diphenylphosphinomethyl)ethane, D-H_2pen = D-penicillamine),[9] we have recently synthesized a unique $Au^{I}_{72}Cd^{II}_{40}Na^{I}_{4}$ 116-nuclear complex, $[Na_4Cd_4\{Cd_3(L^{Au3})_2\}_{12}](NO_3)_{12}$ (**1**$_{\mathbf{CdNa}}$), in which 12 $Au^{I}_6Cd^{II}_3$ cage-type molecules of $[Cd^{II}_3(L^{Au3})_2]$ are linked by 4 Na^{I} and 4 Cd^{II} atoms in a large cage-of-cage structure.[9f] We found that all the Na^{I} and Cd^{II} centres in **1**$_{\mathbf{CdNa}}$ were replaced by Cu^{II} ions to produce $[Cu_8\{Cu_3(L^{Au3})_2\}_{12}](NO_3)_{16}$ with retention of the single crystallinity by soaking the crystals of **1**$_{\mathbf{CdNa}}$ in aqueous $Cu(NO_3)_2$ for 30 minutes. Unfortunately, no intermediate states were detected in this SCSC transformation process because the reactions were very quick with the hetero-epitaxial intermediate state of the crystals. In this study, we report that soaking crystals of **1**$_{\mathbf{CdNa}}$ in aqueous $Co(NO_3)_2$, instead of $Cu(NO_3)_2$, also causes the complete exchange of the Na^{I} and Cd^{II} centres in **1**$_{\mathbf{CdNa}}$ by Co^{II} with retention of the single crystallinity, forming an isostructural 116-nuclear cage-of-cage structure in $[Co_8\{Co_3(L^{Au3})_2\}_{12}](NO_3)_{16}$ (**1**$_{\mathbf{Co}}$). Notably, the SCSC transformation using $Co(NO_3)_2$ was found to proceed much more slowly than that using $Cu(NO_3)_2$ in a homogeneous process (Scheme 1), which allowed us to determine several intermediate states via single crystal X-ray crystallography. To our knowledge, this is the first X-ray snapshot of the intermediate species that exist in the course of the SCSC transmetallation process.

Colourless crystals of **1**$_{\mathbf{CdNa}}$ with a cubic shape were soaked in a 1 M aqueous solution of $Co(NO_3)_2$ at room temperature, affording purple crystals (**1**$_{\mathbf{Co}}$) after 6 days while maintaining their crystal shape and crystallinity. Compound **1**$_{\mathbf{Co}}$ exhibited nearly the same powder X-ray diffraction pattern as **1**$_{\mathbf{CdNa}}$ (Fig. S1, ESI†). The IR spectrum of **1**$_{\mathbf{Co}}$ was also the same as that of **1**$_{\mathbf{CdNa}}$ (Fig. S2, ESI†). However, **1**$_{\mathbf{Co}}$ contains Au and Co atoms as metal components with a lack of Na and Cd atoms, which was confirmed by X-ray fluorescence spectrometry. The diffuse reflection and CD spectral features of **1**$_{\mathbf{Co}}$ in the solid state are reminiscent of those of the previously reported $Au^{I}_6Co^{II}_3$ cage-type complex, $[Co^{II}_3(L^{Au3})_2]$,[9e] in which three Co^{II} centres are coordinated by two L^{Au3} metalloligands in a *cis*(N)·*trans*(O)·*cis*(S) octahedral geometry (Fig. S3, ESI†). Thus, it is considered that the Na^{I} and Cd^{II} atoms in **1**$_{\mathbf{CdNa}}$ were completely replaced by Co^{II} atoms to produce **1**$_{\mathbf{Co}}$.

The structure of **1**$_{\mathbf{Co}}$ was established by single-crystal X-ray analysis (Table S1). **1**$_{\mathbf{Co}}$ crystallized in the cubic space group of *F*432 with unit cell parameters of a = 76.541 Å and V = 448,417 Å^3, which are essentially the same as those of **1**$_{\mathbf{CdNa}}$ (a = 77.714 Å, V = 469,342 Å^3). This implies that the conversion of **1**$_{\mathbf{CdNa}}$ to **1**$_{\mathbf{Co}}$ proceeded in an SCSC transformation manner. The asymmetric unit of **1**$_{\mathbf{Co}}$ contains an entire $Au^{I}_6Co^{II}_3$ cage-type molecule of $[Co^{II}_3(L^{Au3})_2]$ that is connected by two Co^{II} atoms through carboxylate groups (Figs. 1a, 1b and S4, ESI†).

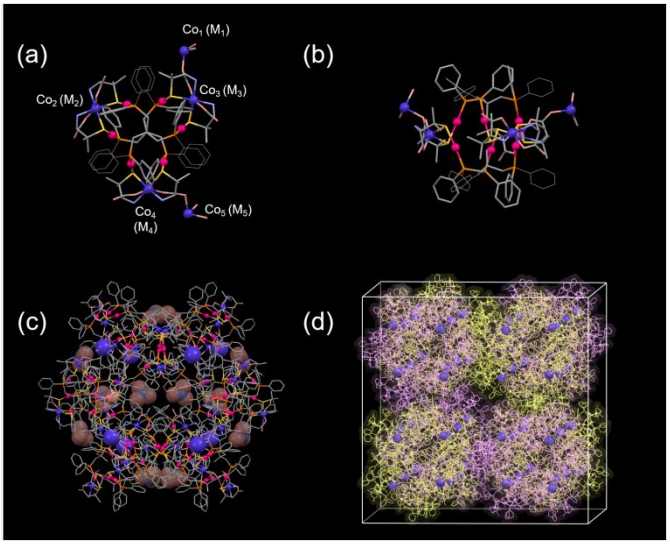

Fig. 1. Crystal structures of **1**$_{\mathbf{Co}}$. (a) Top and (b) side views of the $[Co^{II}_3(L^{Au3})_2]$ molecule with linking Co^{II} atoms. (c) The entire $Au^{I}_{72}Co^{II}_{44}$ cage-of-cage with NO_3^- anions. (d) The packing of the cage-of-cage molecules (cream and pink). Colour codes: red, Au; violet, Co; orange, P; yellow, S; pink, O; pale blue, N; grey, C.

Thus, not only Na^{I} and Cd^{II} atoms that link the $[Co^{II}_3(L^{Au3})_2]$ molecules but also all the Cd^{II} atoms that are surrounded by two tridentate-N,O,S D-pen ligands in **1**$_{\mathbf{CdNa}}$ (Fig. S5, ESI†) were replaced by Co^{II} atoms in **1**$_{\mathbf{Co}}$. In **1**$_{\mathbf{Co}}$, 8 Co^{II} atoms are arranged in a distorted cube, with each of the 12 sides of the cube being occupied by the $[Co^{II}_3(L^{Au3})_2]$ molecule such that each Co^{II} atom connects 3 $[Co^{II}_3(L^{Au3})_2]$ molecules (Fig. S6, ESI†). This connection generates a cationic 116-nuclear $Au^{I}_{72}Co^{II}_{44}$ cage-of-cage structure in $[Co_8\{Co_3(L^{Au3})_2\}_{12}]^{16+}$ (Fig. 1c), which is isostructural with the $Au^{I}_{72}Cd^{II}_{40}Na^{I}_{4}$ structure in **1**$_{\mathbf{CdNa}}$ (Figs. S6 and S7, ESI†). As in the case of **1**$_{\mathbf{CdNa}}$, 12 nitrate anions are located on the surface of the cage-of-cage of **1**$_{\mathbf{Co}}$, with each nitrate anion connecting 3 $[Co^{II}_3(L^{Au3})_2]$ molecules through CH···O interactions (Figs. 1c and S6), which appears to sustain the cage-of-cage in the course of the SCSC transformation from **1**$_{\mathbf{CdNa}}$ to **1**$_{\mathbf{Co}}$.

Each Co^{II} centre in the $[Co^{II}_3(L^{Au3})_2]$ molecule in **1**$_{\mathbf{Co}}$ has a *cis*(N)·*trans*(O)·*cis*(S) octahedral geometry coordinated by two tridentate-N,O,S D-pen ligands (Fig. 1a), as in the case of each Cd^{II} centre in **1**$_{\mathbf{CdNa}}$ (Fig. S5, ESI†). The bond distances around the Co^{II} centres in **1**$_{\mathbf{Co}}$ (average: Co-S = 2.45 Å, Co-O = 2.09 Å, Co-N = 2.15 Å; Table S2) are considerably shorter than the corresponding distances around the Cd^{II} centres in **1**$_{\mathbf{CdNa}}$ (av. Cd-S = 2.64 Å, Cd-O = 2.37 Å, Cd-N = 2.33 Å) and are comparable to those found in the discrete $[Co^{II}_3(L^{Au3})_2]$ complex (average: Co-S = 2.49 Å, Co-O = 2.12 Å, Co-N = 2.14 Å)[9f].‡ The bond distances between the linking Co^{II} atoms and the carboxyl O atoms from the $[Co^{II}_3(L^{Au3})_2]$ molecules in **1**$_{\mathbf{Co}}$ (Co1-O = 2.08 Å, Co5-O = 2.13 Å) are also shorter than those between the linking Na^{I} and Cd^{II} atoms and the carboxyl O atoms from the $[Cd^{II}_3(L^{Au3})_2]$ molecules in **1**$_{\mathbf{CdNa}}$ (av. Na1-O = 2.23 Å, Cd5-O = 2.24 Å). Thus, the replacement of Na^{I} and Cd^{II} atoms in **1**$_{\mathbf{CdNa}}$ by Co^{II} atoms led to the formation of a more rigid cage-of-cage structure in **1**$_{\mathbf{Co}}$.§

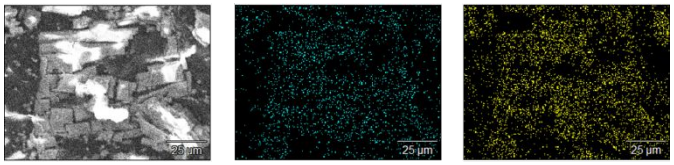

Fig. 2. (left) SEM image and the EDS element mappings of (middle) Co and (right) Cd atoms of crystals after soaking $\mathbf{1}_{\mathbf{CdNa}}$ in aqueous $Co(NO_3)_2$ for 2 days.

We noticed that the colourless crystals gradually and homogeneously became pale purple and then purple in the course of the transformation from $\mathbf{1}_{\mathbf{CdNa}}$ to $\mathbf{1}_{\mathbf{Co}}$ (Scheme 1). The homogeneity of the intermediate crystals was shown by SEM-EDX spectroscopy, which revealed the homogeneous distribution of Co and Cd atoms in the crystal (Fig. 2). The gradual increase in the total amount of Co atoms over the course of the transformation process was confirmed by X-ray fluorescence analysis (Fig. S8, ESI†), together with diffuse reflection spectroscopy (Fig. S9, ESI†). The homogeneous nature of the transformation inspired us to determine the intermediate states of crystals via single-crystal X-ray diffraction measurements. We selected a series of single crystals that were soaked in a 1 M aqueous solution of $Co(NO_3)_2$ for 1 hour ($\mathbf{1}^{\mathbf{1h}}$), 6 hours ($\mathbf{1}^{\mathbf{6h}}$), 1 day ($\mathbf{1}^{\mathbf{1d}}$), 2 days ($\mathbf{1}^{\mathbf{2d}}$), and 4 days ($\mathbf{1}^{\mathbf{4d}}$) as intermediate species. While all the crystals $\mathbf{1}^{\mathbf{1h}}$, $\mathbf{1}^{\mathbf{6h}}$, $\mathbf{1}^{\mathbf{1d}}$, $\mathbf{1}^{\mathbf{2d}}$, and $\mathbf{1}^{\mathbf{4d}}$ were found to possess a 116-nuclear cage-of-cage structure that is essentially the same as the structures of $\mathbf{1}_{\mathbf{CdNa}}$ and $\mathbf{1}_{\mathbf{Co}}$ (Table S1), the electron densities at metal centres (M_1 and M_5 in the linker sites and M_2, M_3, and M_4 in the $[M^{II}_3(L^{Au3})_2]$ cage molecule) were different, and thus, each metal centre was refined as a positional disordered of two kinds of metal atoms (Na^I/Co^{II} or Cd^{II}/Co^{II}) with variable site occupancies (Table S3).

As shown in Fig. 3, the site occupancies of Co^{II} for each metal centre commonly increase with increasing soaking time, but the rates of increase are highly dependent on the metal centres. The first metal replacement by Co^{II} occurred at the M_1 site occupied by the Na^I atom in $\mathbf{1}_{\mathbf{CdNa}}$, which was completed after 1 h of soaking time ($\mathbf{1}^{\mathbf{1h}}$) to be refined as a Co atom, while each of the M_2, M_3, M_4, and M_5 sites in $\mathbf{1}^{\mathbf{1h}}$ was still occupied by Cd^{II}. This was expected because the Na^I centre in $\mathbf{1}_{\mathbf{CdNa}}$ is weakly bound by three carboxyl O atoms from three $[Cd^{II}_3(L^{Au3})_2]$ molecules (Fig. S7, ESI†). One may assume that the Cd^{II} centre of the M_5 site, which is coordinated by three carboxyl O atoms from three $[Cd^{II}_3(L^{Au3})_2]$ molecules (Fig. S7, ESI†), would be more easily replaced by Co^{II} than the other Cd^{II} centres of the M_2, M_3, and M_4 sites, which are each surrounded by two tridentate-N,O,S D-pen ligands in the $[Cd^{II}_3(L^{Au3})_2]$ cage molecule (Fig. S5, ESI†). However, the Co/Cd occupancy values commonly decrease in the order $M_2 > M_3 > M_5 > M_4$ in $\mathbf{1}^{\mathbf{6h}}$, $\mathbf{1}^{\mathbf{1d}}$, and $\mathbf{1}^{\mathbf{2d}}$ (Fig. 3). In $\mathbf{1}^{\mathbf{4d}}$, each metal site was almost completely refined as Co, although the M_4 site was only slightly occupied by Cd, which was fully replaced by Co after 6 days. A detailed inspection of the crystal structure in $\mathbf{1}_{\mathbf{CdNa}}$ revealed that the metal centre of the M_2 site is exposed to the surface of the cage-of-cage to be easily attacked by external aqua Co^{II} species (Fig. S10, ESI†). This

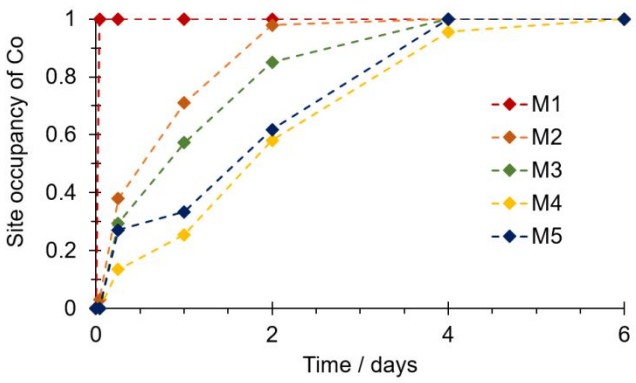

Fig. 3. Time-dependent changes in the site occupancies of the Co^{II} atom of metal centres (M_1, M_2, M_3, M_4, M_5) determined by single-crystal X-ray diffraction analysis.

appears to be responsible for the second easiest replacement by Co^{II} of M_2 site. The easier replacement of the Cd^{II} centre at the M_3 site relative to the M_5 site is explained by weaker binding of the bridging carboxylate to the Cd^{II} centre of the M_3 site, which is induced by the replacement of Na^I by Co^{II} at the M_1 site. The slowest metal replacement by Co^{II} occurred at the Cd^{II} atom of the M_4 site in the $[Cd^{II}_3(L^{Au3})_2]$ molecule, which is connected by the linking Cd^{II} atom of the M_5 site (Fig. S7, ESI†). Note that the replacement rates of the metal centres of the M_4 and M_5 sites are relatively close to each other (Fig. 3). This is also the case for the metal centres of the M_2 and M_3 sites. Thus, $\mathbf{1}_{\mathbf{CdNa}}$ is homogeneously converted to $\mathbf{1}_{\mathbf{Co}}$ by way of intermediate states that can be best represented as $[Co_4Cd_4\{Cd_3(L^{Au3})_2\}_{12}]^{16+}$ and $[Co_4Cd_4\{Co_2Cd(L^{Au3})_2\}_{12}]^{16+}$ (Fig. 4 and S11, ESI†).

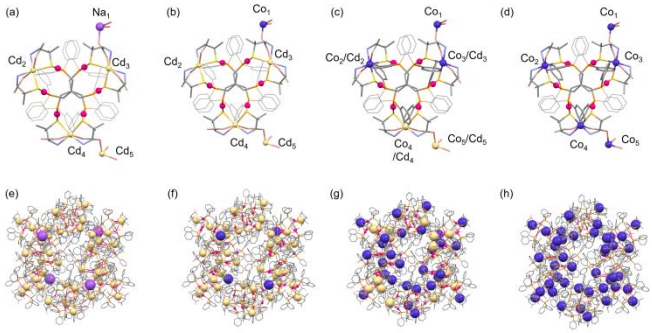

Fig. 4. Crystal structures of (a-d) the asymmetric units and (e-h) the cage-of-cage molecules in $\mathbf{1}_{\mathbf{NaCd}}$, $\mathbf{1}^{\mathbf{1h}}$, $\mathbf{1}^{\mathbf{1d}}$, and $\mathbf{1}_{\mathbf{Co}}$. (a) $\mathbf{1}_{\mathbf{NaCd}}$. (b) $\mathbf{1}^{\mathbf{1h}}$. (c) $\mathbf{1}^{\mathbf{1d}}$: Co^{II} and Cd^{II} atoms are disordered at M_2, M_3, M_4, and M_5 metal centres with site occupancies of 0.71/0.29 for M_2, 0.57/0.43 for M_3, 0.25/0.75 for M_4, and 0.33/0.67 for M_5, respectively. (d) $\mathbf{1}_{\mathbf{Co}}$. Colour codes: red, Au; cream, Cd; purple, Na; violet, Co; orange, P; yellow, S; pink, O; pale blue, N; grey, C.

The SCSC transformation of $\mathbf{1}_{\mathbf{CdNa}}$ to $\mathbf{1}_{\mathbf{Co}}$ is thanks to the presence of large interstices (diameters of ~3.1 nm) connected by porous channels (minimum diameter ~5 Å) in $\mathbf{1}_{\mathbf{CdNa}}$ (Fig. S12, ESI†), which permits the smooth migration and accommodation of aqua Co^{II} species inside the crystal. The presence of a considerable number of aqua Co^{II} species in the crystals of $\mathbf{1}^{\mathbf{1h}}$, $\mathbf{1}^{\mathbf{6h}}$, $\mathbf{1}^{\mathbf{1d}}$, $\mathbf{1}^{\mathbf{2d}}$, $\mathbf{1}^{\mathbf{4d}}$, and $\mathbf{1}_{\mathbf{Co}}$ was confirmed by X-ray fluorescence (Fig. S8, ESI†) and elemental analysis, although the positions of aqua Co^{II} species were not determined by single-crystal X-ray

analysis. The rigidity of the crystal framework in $\mathbf{1_{CdNa}}$, in which the cage-of-cage molecules are closely packed in a pseudo-primitive cubic lattice through CH···π and π ··· π interactions (Fig. S13, ESI†), is also critical to the transformation that proceeds in an SCSC manner. Notably, the SCSC transformation from $\mathbf{1_{CdNa}}$ to $\mathbf{1_{Co}}$ proceeded gradually and homogeneously over 6 days. This is distinct from the quick transformation of $\mathbf{1_{CdNa}}$ to $[Cu_8\{Cu_3(L^{Au3})_2\}_{12}](NO_3)_{16}$,[9f] which was completed within 30 minutes under the same conditions.¶ It is reasonable to assume that the migration and accommodation of aqua Co^{II} species inside the crystal complete before the occurrence of the metal replacement because of the rate constant of the exchange of coordinated water molecules in aqua Co^{II} species, which is much slower than that in aqua Cu^{II} species.[10] Thus, the slower exchange rate for aqua Co^{II} species, as well as the accommodation of a large amount of aqua Co^{II} species inside the crystal, is most likely responsible for the homogeneous SCSC transformation from $\mathbf{1_{CdNa}}$ to $\mathbf{1_{Co}}$. Here, it should be noted that attempts to prepare $\mathbf{1_{Co}}$ by the direct reaction of H_3L^{Au3} and $Co(NO_3)_2$ were unsuccessful, producing only the $Au^{I}_6Co^{II}_3$ nonanuclear complex, $[Co^{II}_3(L^{Au3})_2]$.[9e]

In summary, we showed in this study that the $Au^{I}_{72}Cd^{II}_{40}Na^{I}_4$ cage-of-cage of $[Na_4Cd_4\{Cd_3(L^{Au3})_2\}_{12}](NO_3)_{12}$ ($\mathbf{1_{NaCd}}$) is converted to the analogous $Au^{I}_{72}Co^{II}_{44}$ cage-of-cage of $[Co_8\{Co_3(L^{Au3})_2\}_{12}](NO_3)_{16}$ ($\mathbf{1_{Co}}$) with retention of the single crystallinity by soaking its crystals in aqueous $Co(NO_3)_2$, accompanied by the replacement not only of the linking Na^{I} and Cd^{II} atoms but also of the Cd^{II} atoms in the $[Cd_3(L^{Au3})_2]$ molecules. Importantly, the SCSC transformation proceeded gradually and homogeneously, which allowed us to observe intermediate states by the X-ray snapshot technique for the first time. This is due to the moderate exchange rate of water molecules in aqua Co^{II} species, together with the smooth inclusion and accommodation of a large amount of aqua Co^{II} species inside the crystal that possesses large interstices connected by porous channels in a rigid framework structure. The findings of this study will provide new mechanistic insight into the observation of intermediate species not only for metal exchange reactions but also for other chemical reactions in the crystalline state.

This work was supported by JST CREST (Grant No. JPMJCR13L3) and JSPS KAKENHI (Grant Nos. 18H05344 and 20K05664). The synchrotron radiation experiments were performed at 2D-SMC of the Pohang Accelerator Laboratory.

Notes and references

‡ It is assumed that a flexible nature of the tripodal tdme ligand compensates the shorter Co-O/N bond distances to give the cage-of-cage molecule in $\mathbf{1_{Co}}$, the size of which is similar to that of the cage-of-cage molecule in $\mathbf{1_{CdNa}}$, leading to the cell parameters of $\mathbf{1_{Co}}$ essentially the same as those of $\mathbf{1_{CdNa}}$.

§ Soaking crystals of $\mathbf{1_{Co}}$ in 1 M aqueous $Cd(NO_3)_2$ for 7 days did not cause the exchange of Co^{II} atoms in $\mathbf{1_{Co}}$ by Cd^{II} atoms, which was confirmed by X-ray fluorescence analysis.

¶ Soaking crystals of $\mathbf{1_{CdNa}}$ in 1 M aqueous $FeCl_2$ or $Ni(NO_3)_2$ resulted in the loss of their single-crystallinity. While the single-crystallinity was retained on soaking crystals of $\mathbf{1_{CdNa}}$ in 1 M aqueous $Zn(NO_3)_2$ or $Mn(NO_3)_2$, the metal exchange event was not completed even after 2 weeks, which was shown by X-ray fluorescence analysis, together with single-crystal X-ray crystallography (Fig. S14, ESI†).

1 (a) K. K. Tanabe and S. M. Cohen, *Chem. Soc. Rev.*, 2011, **40**, 498; (b) J. P. Zhang, P. Q. Liao, H. L. Zhou, R. B. Lin and X. M. Chen, *Chem. Soc. Rev.*, 2014, **43**, 5789; (c) P. Deria, J. E. Mondloch, O. Karagiaridi, W. Bury, J. T. Hupp and O. K. Farha, *Chem. Soc. Rev.*, 2014, **43**, 5896; (d) J. D. Evans, C. J. Sumby and C. J. Doonan, *Chem. Soc. Rev.*, 2014, **43**, 5933.

2 (a) W. M. Bloch, A. Burgun, C. J. Coghlan, R. Lee, M. L. Coote, C. J. Doonan and C. J. Sumby, *Nat. Chem.*, 2014, **6**, 906; (b) W. M. Bloch, N. R. Champness and C. J. Doonan, *Angew. Chem., Int. Ed.*, 2015, **54**, 12860; (c) T. L. Easun, F. Moreau, Y. Yan, S. Yang and M. Schröder, *Chem. Soc. Rev.*, 2017, **46**, 239.

3 (a) Y. Inokuma, M. Kawano and M. Fujita, *Nat. Chem.*, 2011, **3**, 349–358; (b) Y. Ohashi, *Crystalline State Photoreactions*, Springer, Japan, 2014; (c) J. J. Vittal and H. S. Quah, *Dalton Trans.*, 2017, **46**, 7120; (d) W. W. He, S. L. Li and Y. Q. Lan, *Inorg. Chem. Front.*, 2018, **5**, 279; (e) Z. Yin, S. Wan, J. Yang, M. Kurmoo and M.-H. Zeng, *Coord. Chem. Rev.*, 2019, **378**, 500; (f) L.E. Hatcher, M.R. Warren, A.R. Pallipurath, L.K. Saunders and J.M. Skelton, *Watching Photochemistry Happen: Recent Developments in Dynamic Single-Crystal X-Ray Diffraction Studies*. Springer, Berlin, Heidelberg, 2020.

4 (a) M. R. Warren, S. K. Brayshaw, A. L. Johnson, S. Schiffers, P. R. Raithby, T. L. Easun, M. W. George, J. E. Warren and S. J. Teat, *Angew. Chem., Int. Ed.*, 2009, **48**, 5711; (b) C. W. Machan, A. M. Lifschitz, C. L. Stern, A. A. Sarjeant, and C. A. Mirkin, *Angew. Chem.* 2012, **124**, 1498; (c) F. L. Hu, S. L. Wang, J. P. Lang and B. F. Abrahams, *Sci. Rep.*, 2014, **4**, 6815.

5 (a) B. Li, R. J. Wei, J. Tao, R. B. Huang, L. S. Zheng and Z. P. Zheng, *J. Am. Chem. Soc.*, 2010, **132**, 1558; (b) G. Aromí, C. M. Beavers, J. Sánchez Costa, G. A. Craig, G. Mínguez Espallargas, A. Orera and O. Roubeau, *Chem. Sci.*, 2016, **7**, 2907.

6 (a) R. Kubota, S. Tashiro, M. Shiro and M. Shionoya, *Nat. Chem.*, 2014, **6**, 913; (b) P. Shen, W.-W. He, D.-Y. Du, H.-L. Jiang, S.-L. Li, Z.-L. Lang, Z.-M. Su, Q. Fua and Y.-Q. Lan, *Chem. Sci.*, 2014, **5**, 1368.

7 (a) T. Kawamichi, T. Haneda, M. Kawano and M. Fujita, *Nature*, 2009, **461**, 633; (b) Y.-S. Wei, M. Zhang, P.-Q. Liao, R.-B. Lin, T.-Y. Li, G. Shao, J.-P. Zhang and X.-M. Chen, *Nat. Commun.*, 2015, **6**, 8348.

8 (a) S. Das, H. Kim and K. Kim, *J. Am. Chem. Soc.*, 2009, **131**, 3814; (b) X. Song, T. K. Kim, H. Kim, D. Kim, S. Jeong, H. R. Moon and M. S. Lah, *Chem. Mater.*, 2012, **24**, 3065; (c) M. Lalonde, W. Bury, O. Karagiaridi, Z. Brown, J. T. Hupp and O. K. Farha, *J. Mater. Chem. A*, 2013, **1**, 5453; (d) Z. Zhang, L. Wojtas, M. Eddaoudi and M. J. Zaworotko, *J. Am. Chem. Soc.*, 2013, **135**, 5982; (e) W. Meng, H. Li, Z. Xu, S. Du, Y. Li, Y. Zhu, Y. Han, H. Hou, Y. Fan and M. Tang, *Chem. – Eur. J.*, 2014, **20**, 2945; (f) Y. Han, J. R. Li, Y. Xie and G. Guo, *Chem. Soc. Rev.*, 2014, **43**, 5952; (g) C. K. Brozeka and M. Dinca, *Chem. Soc. Rev.*, 2014, **43**, 5456; (h) T. Grancha, J. Ferrando-Soria, H.-C. Zhou, J. Gascon, B. Seoane, J. Pasán, O. Fabelo, M. Julve and E. Pardo, *Angew. Chem., Int. Ed.*, 2015, **54**, 6521; (i) M.-M. Xu, Q. Chen, L.-H. Xie and J.-R. Li, *Coord. Chem. Rev.*, 2020, **421**, 213421.

9 (a) N. Yoshinari and T. Konno, *Chem. Rec.*, 2016, **16**, 1647; (b) S. Yamashita, Y. Nakazawa, S. Yamanaka, M. Okumura, T. Kojima, N. Yoshinari and T. Konno, *Sci. Rep.*, 2018, **8**, 2606; (c) N. Yoshinari and T. Konno, *Bull. Chem. Soc. Jpn.*, 2018, **91**, 790; (d) Yoshinari, N.; Konno, T. Coordination Molecular Technology. In *Molecular Technology*, Vol. 4: Synthesis Innovation; Yamamoto, H.; Kato, T., Eds.; Wiley–VCH: Weinheim, Germany, 2019; 199; (e) Y. Hashimoto, N. Yoshinari, N. Matsushita and T. Konno, *Eur. J. Inorg. Chem.*, 2014, 3474; (f) K. Imanishi, B. Wahyudianto, T. Kojima, N. Yoshinari, and T. Konno, *Chem. Eur. J.*, 2020, **26**, 1827.

10 (a) M. Eigen, *Pure Appl. Chem.*, 1963, **6**, 97; (b) H. Ohtaki, *Chem. Rev.*, 1993, **93**, 1157.